Supplementary Information for

Macroscopic and Microscopic Defect Management in Blue/Green Photodetectors for Underwater Wireless Optical Communication

Xiangyu Zhou,[ab] Lingzhi Luo,[b] Yixuan Huang,[b] Shunyong Wei,[b] Jihua Zou,[b] Aoxi He,[c] Binbin Huang,[d] Xiao Li,[e] Junting Zhao,*[f] Kai Shen,*[b] Dewei Zhao*[c] and Jiang Wu[b]

[a] College of Chemistry and Chemical Engineering, Henan University of Technology, Zhengzhou 450001, China

[b] Institute of Fundamental and Frontier Sciences, University of Electronic Science and Technology of China, Chengdu 610054, China

[c] College of Materials Science and Engineering & Institute of New Energy and Low-Carbon Technology, Sichuan University, Engineering Research Center of Alternative Energy Materials & Devices, Ministry of Education, Chengdu 610065, China

[d] College of Material Science and Engineering, Sichuan University, Chengdu 610065, China

[e] Department of Electronic and Electrical Engineering, University College London Torrington Place, London WC1E 7JE, UK

[f] School of Environmental and Engineering, Henan University of Technology, Zhengzhou 450001, China

Corresponding Authors

*E-mail: kaishen@uestc.edu.cn , dewei_zhao@hotmail.com and dewei.zhao@scu.edu.cn, zjtyjk@126.com

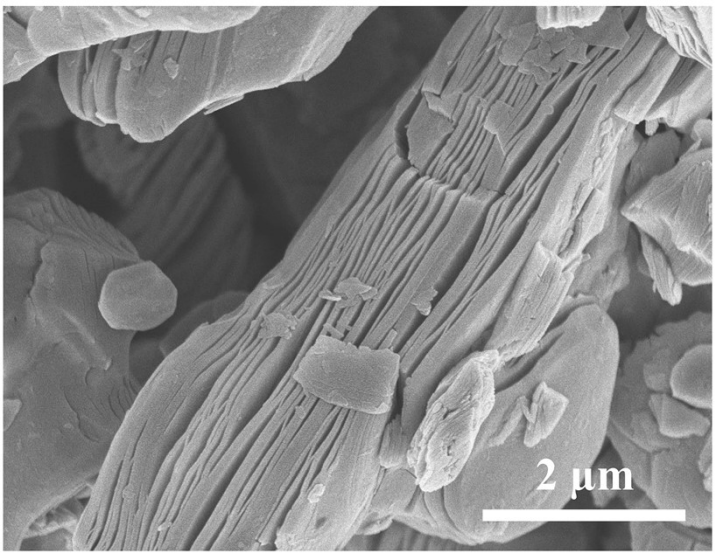

Figure S1. SEM image of pristine multi-layered MXene.

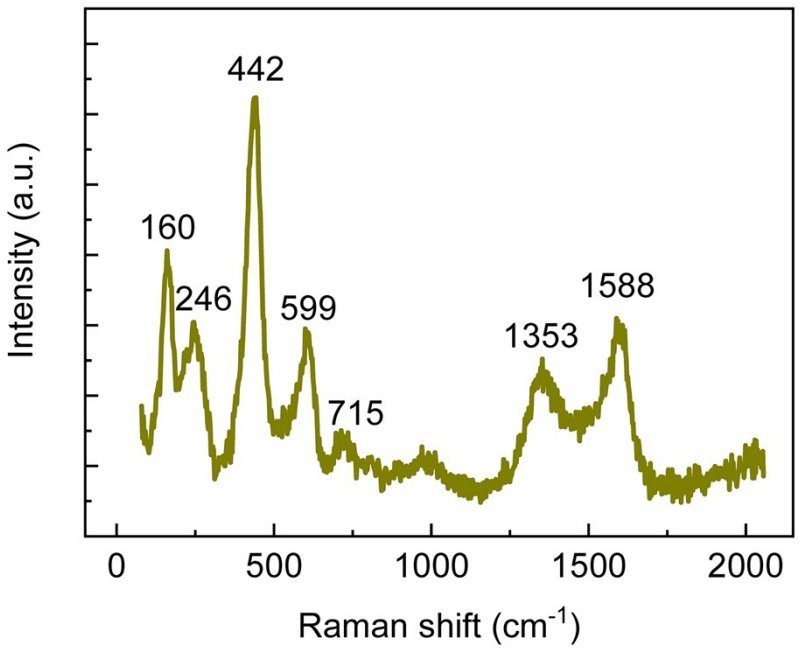

Figure S2. Raman spectrum of Br-terminated Ti_3C_2 MXene nanoparticles.

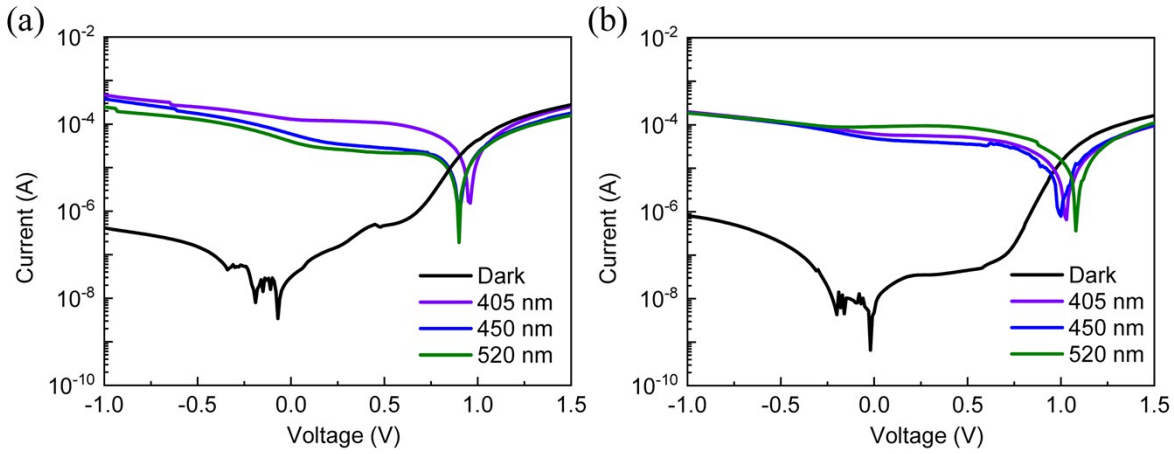

Figure S3. Logarithmic *I-V* curves of (a) the pristine and (b) 4% MNPs-modified photodetectors measured in the dark and under illumination with different wavelengths (405, 450, and 520 nm).

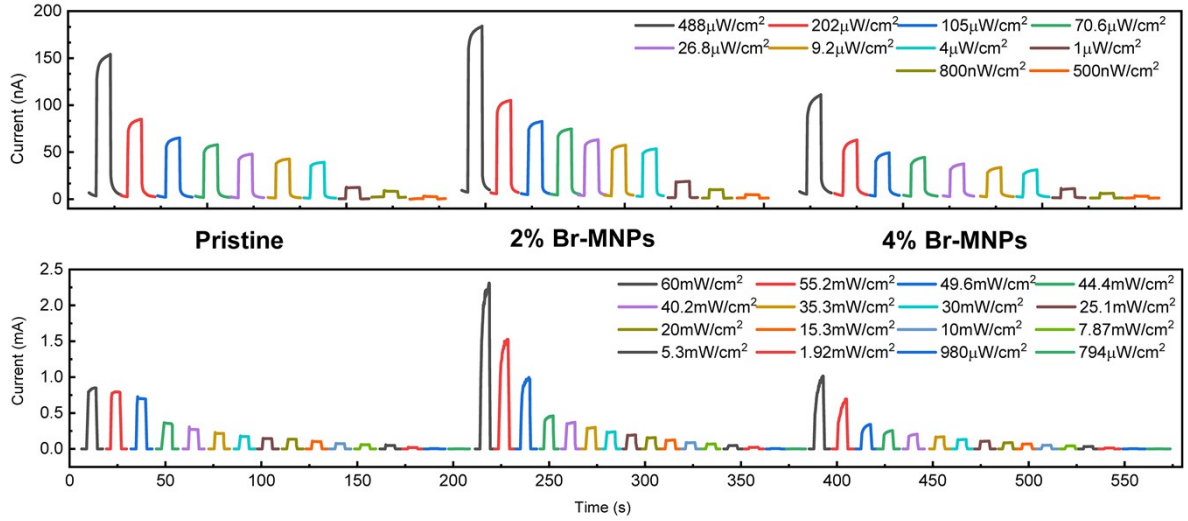

Figure S4. Light intensity-dependent photocurrent of the pristine and MNPs-modified photodetectors measured under 520 nm irradiation with no bias voltage.

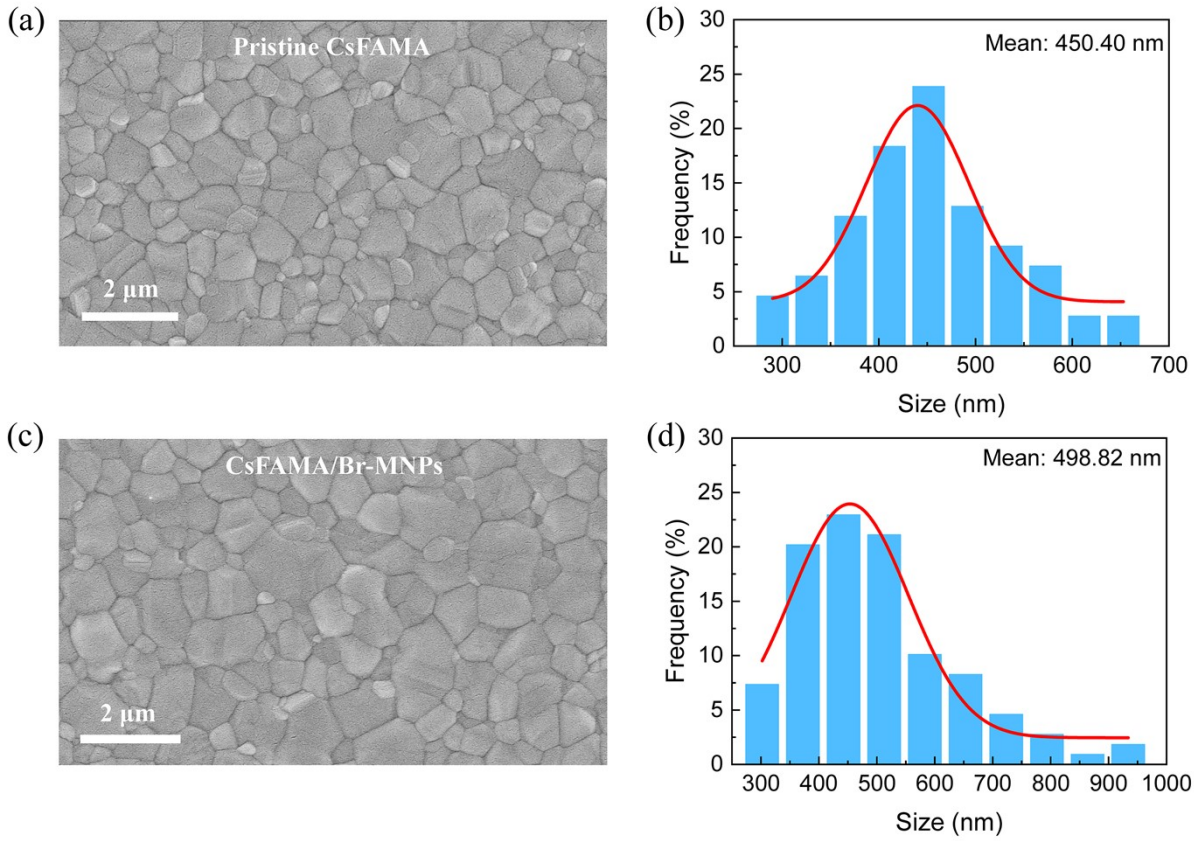

Figure S5. (a) SEM images of the pristine CsFAMA film. (b) The corresponding size distribution. (c) SEM images of CsFAMA film with Br-MNPs. (d) The distribution of corresponding grain size.

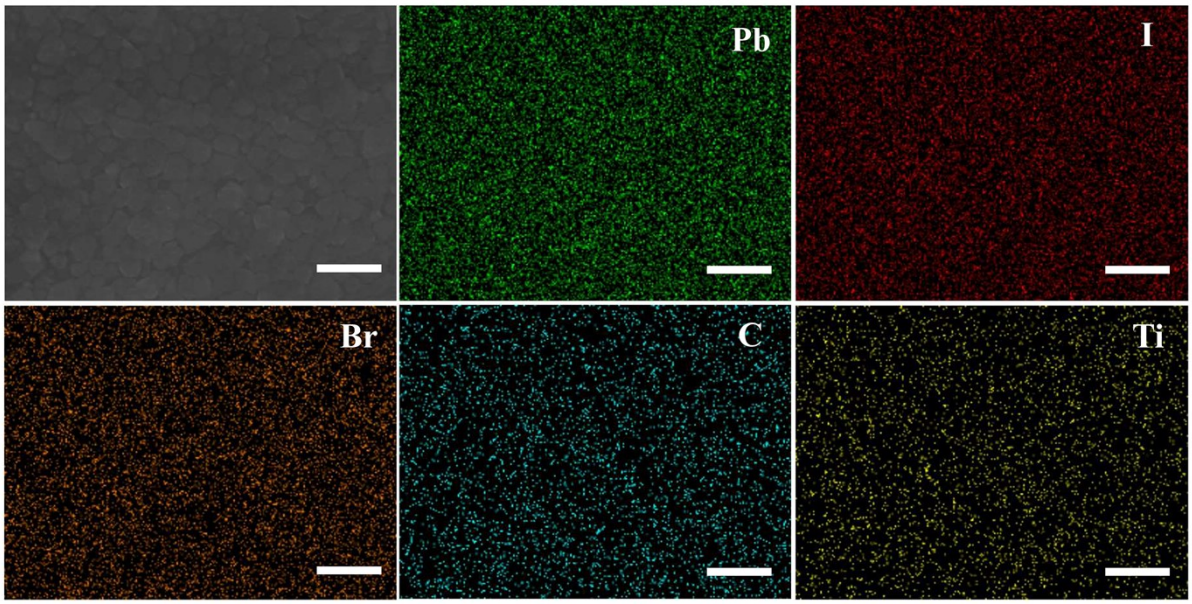

Figure S6. SEM image and the corresponding EDS mapping (Pb, I, Br, C, Ti) of Br-MNPs treated perovskite film. The scale bar is 1 μm.

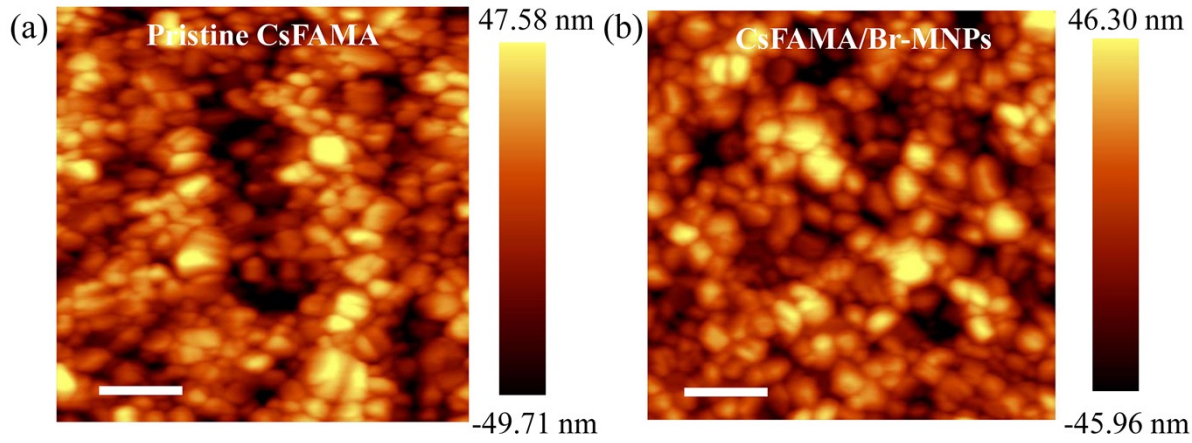

Figure S7. AFM images of (a) pristine and (b) Br-MNPs doped CsFAMA films. Scale bar is 1 μm.

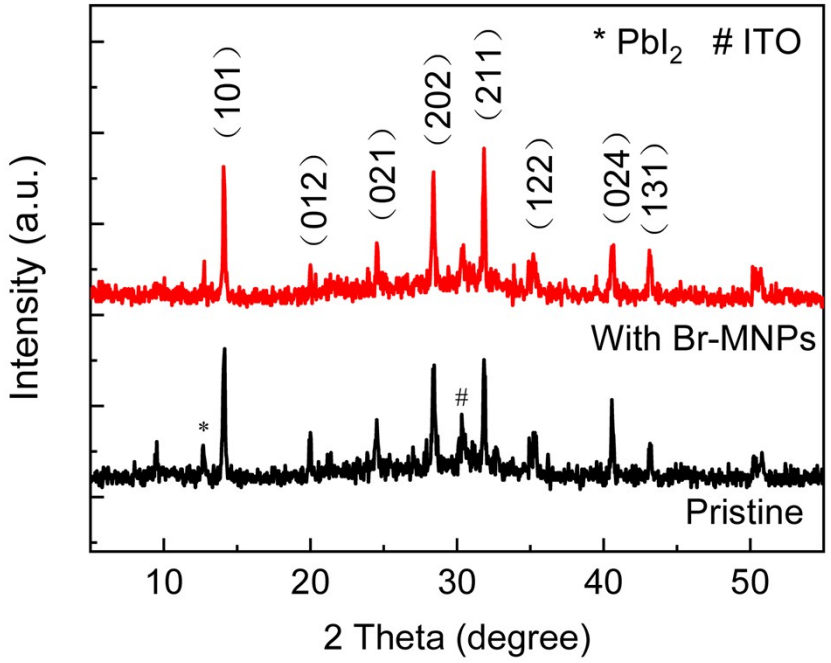

Figure S8. XRD patterns of the perovskite films before and after Br-MNPs treatment.

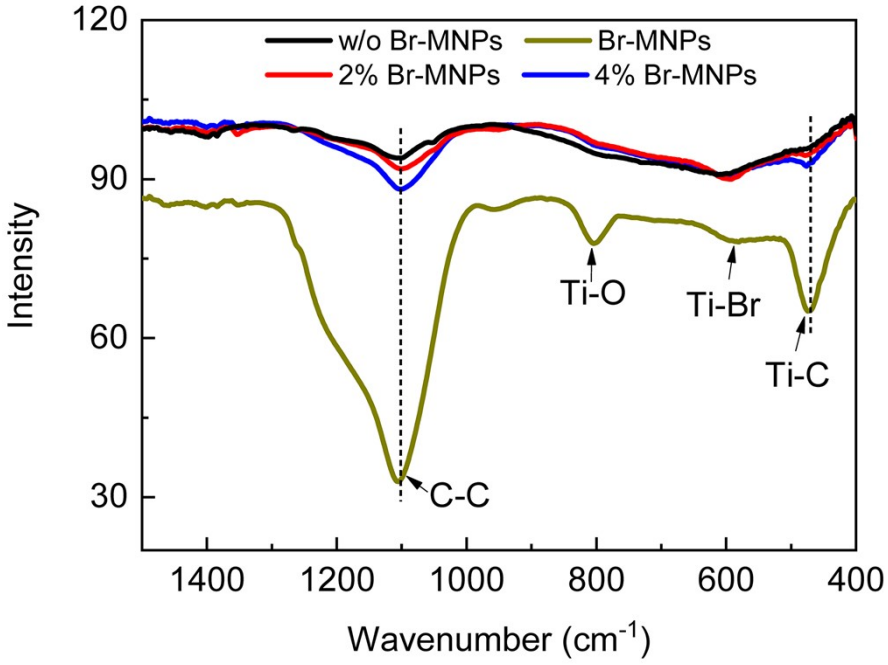

Figure S9. FTIR spectra of the Br-MNPs, pristine perovskite and Br-MNPs assisted perovskite films.

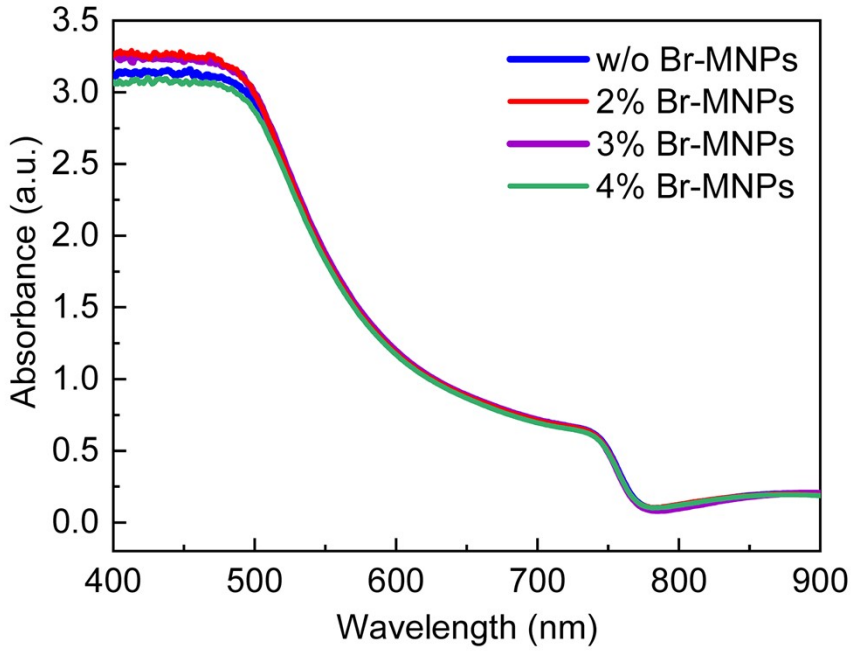

Figure S10. Absorption spectra of different Br-MNPs-assisted perovskite films.

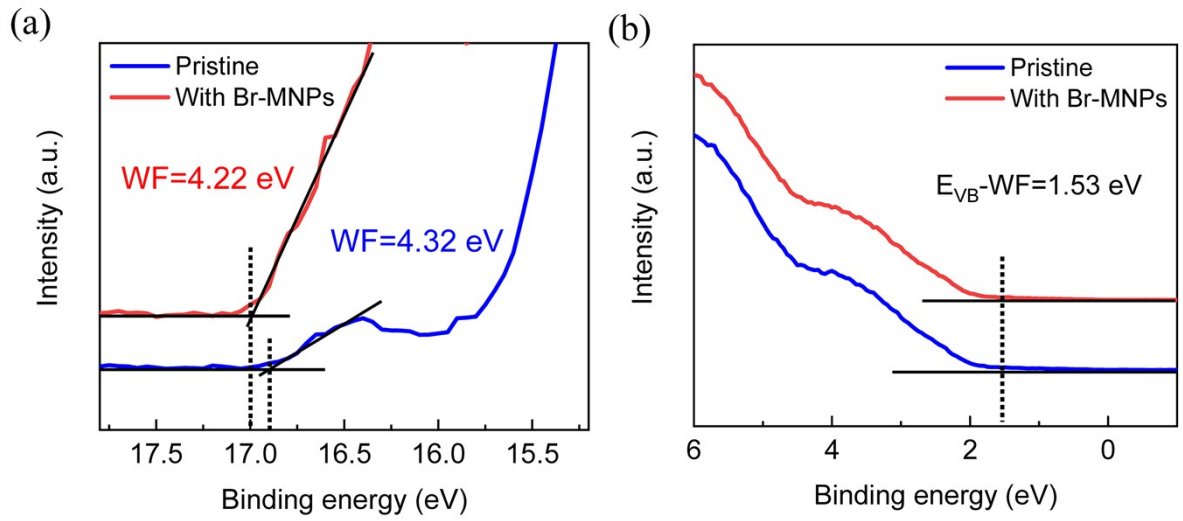

Figure S11. (a) Ultraviolet photoelectron spectroscopy (UPS) spectra of pristine and Br-MNPs decorated perovskite films. The work function (WF) is calculated by the equation: WF = $h\upsilon$ - E_{cutoff}, where E_{cutoff} is the secondary electron cut off. (b) The valance band spectra of both samples.

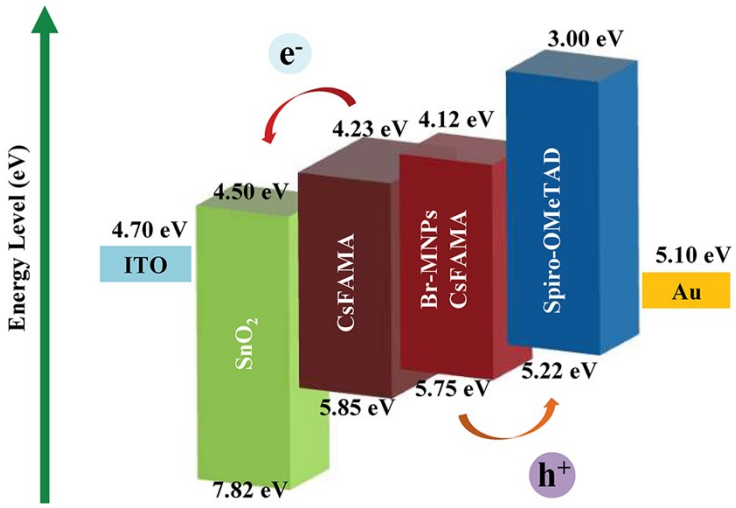

Figure S12. The energy band diagram of the as-fabricated devices.

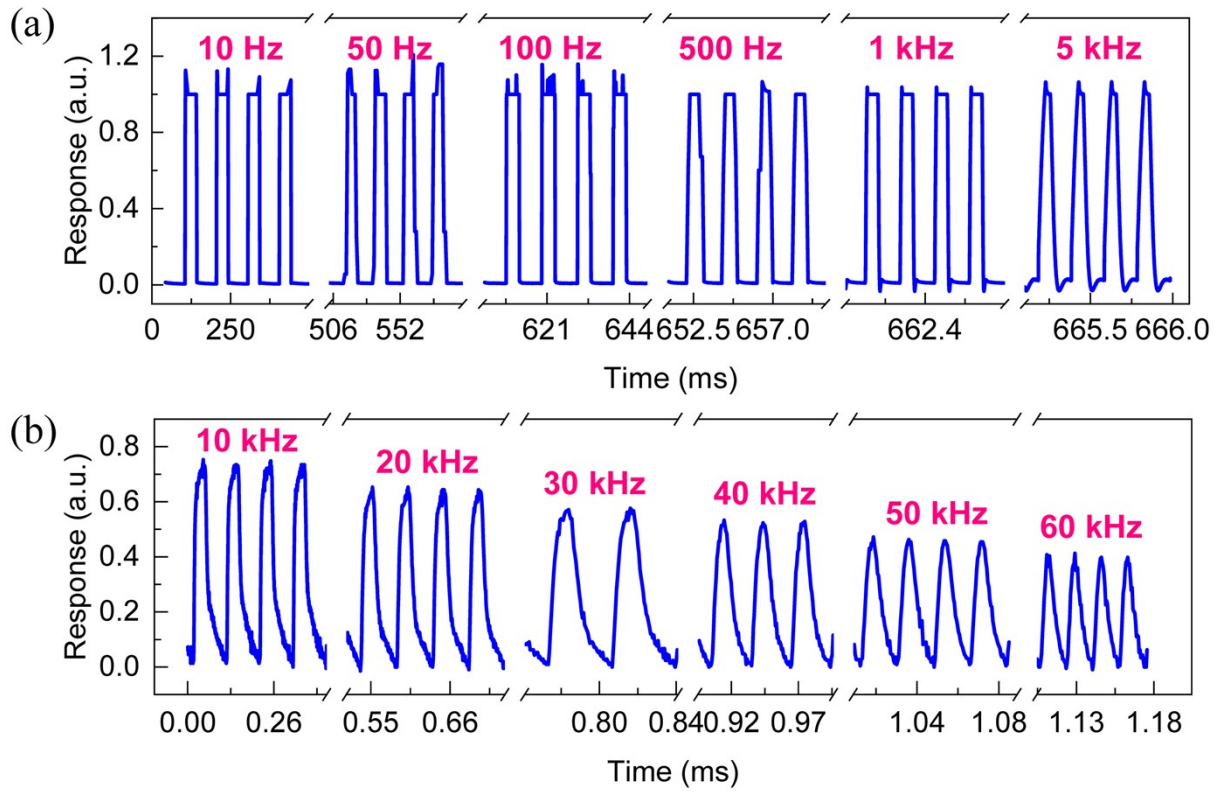

Figure S13. Temporal photoresponse of Br-MNPs assisted photodetector under the pulsed light illumination with modulating frequency from (a) 10 Hz to 5 kHz and (b) 10 kHz to 60 kHz.

Table S1. Surface roughness extracted from AFM results. SA is the root mean square of surface roughness, SQ represents the average value of surface roughness and Peak-Peak denotes the maxima peak height of surface roughness.

Sample	SA (nm)	SQ (nm)	Peak-Peak (nm)
Pristine	17.2	21.4	141
With Br-MNPs	15.6	19.5	136

Table S2. The fitting parameters extracted from PL decay curves using the equation of $I(t) = A_1 exp(-t/\tau_1) + A_2 exp(-t/\tau_2)$.

Sample	τ_1 (ns)	A_1 (%)	τ_2 (ns)	A_2 (%)	τ_{ave} (ns)
Pristine	3.45	26.97	123.43	73.03	122.20
With Br-MNPs	3.25	42.53	80.95	57.47	78.71